Available online at www.sciencedirect.com
SCIENCE DIRECT®
Journal of Non-Crystalline Solids 330 (2003) 156–167
JOURNAL OF NON-CRYSTALLINE SOLIDS
www.elsevier.com/locate/jnoncrysol

Structure and magnetic properties of lead vanadate glasses

A. Mekki [a], G.D. Khattak [a], L.E. Wenger [b,*]

[a] Department of Physics, King Fahd University of Petroleum and Minerals, Dhahran 31261, Saudi Arabia
[b] Department of Physics and Astronomy, Wayne State University, Detroit, MI 48201, USA

Received 27 January 2003

Abstract

X-ray photoelectron spectroscopy (XPS) has been used to obtain structural information on the $x\mathrm{PbO}\cdot(1-x)\mathrm{V_2O_5}$ glass system where $x = 0.22$, 0.35, 0.43, and 0.54. The binding energies from the Pb $4f_{7/2}$ and Pb $4f_{5/2}$ core levels decrease with increasing PbO content while the full-width at half-maximum of these peaks increase. The O 1s spectra show an asymmetry for samples having composition $x < 0.5$, which results from oxygen atoms in the V–O–V configuration (bridging oxygens) and from oxygen atoms in the V–O–Pb and Pb–O–Pb configurations (non-bridging oxygens). The number of non-bridging oxygens was found to increase from 81% to 92% with increasing PbO content. For $x = 0.54$, the O 1s spectrum was symmetric indicating that all three oxygen configurations have essentially the same binding energy. This behavior in addition to the decreasing binding energies of the Pb 4f levels with increasing PbO content suggest that the Pb–O bonds are becoming more covalent in nature and that eventually PbO changed its role from a glass modifier to a glass former for $x > 0.5$. The asymmetric V $2p_{3/2}$ peaks for the $x < 0.4$ glasses indicate the presence of a small concentration of V^{4+} ions in addition to V^{5+} ions, while the symmetric V $2p_{3/2}$ peaks for the more concentrated PbO vanadate glasses indicate only V^{5+} being present. The concentration of V^{4+} ions (0–4%) from the XPS data is consistent with determinations from magnetic susceptibility measurements on the same glass samples. In addition to the paramagnetic contribution (Curie–Weiss temperature-dependent behavior) from the V^{4+} ions, the susceptibility for these oxide glasses consisted of a positive, constant contribution arising from the temperature-independent paramagnetic V_2O_5 exceeding the diamagnetism from the core ions.

1. Introduction

The glass structure of lead oxide glasses is especially interesting since a level of up to 70 mol% of lead oxide can be incorporated in the glass network of binary glasses even though PbO by itself does not form a glass. For example, an early investigation of the local glass structure in lead silicate glasses using X-ray photoelectron spectroscopy (XPS) by Smets and Lommen [1] found that the number of bridging oxygens decreased with increasing PbO content such that PbO behaves as network modifier for PbO $\leqslant$ 0.5 mol%. At higher lead concentration, the number of bridging oxygen decreases less rapidly indicating

* Corresponding author. Present address: University of Alabama at Birmingham (UAB), School of Natural Sciences and Mathematics, Birmingham, AL 35294, USA. Tel.: +1-205 934 5102; fax: +1-205 975 6111.
E-mail address: wenger@uab.edu (L.E. Wenger).

0022-3093/$ - see front matter © 2003 Elsevier B.V. All rights reserved.
doi:10.1016/j.jnoncrysol.2003.08.039

the presence of polymerized silicate anions. More recent studies by Wang and Zhang [2] and Gee et al. [3] on the lead silicate glass system concluded that SiO_2 is the glass former for the low concentration regime (PbO < 40 mol%). The glass former consists of a SiO_4 tetrahedra network while PbO_4 pyramids form a separate network structure. For the high concentration regime (PbO > 40 mol%), the PbO_4 pyramid polymeric chains connect together through the SiO_4 tetrahedra to form the glass structure network. Likewise, the local structure of binary lead vanadate glasses as a function of PbO composition has been investigated by a variety of techniques. For example, infrared spectroscopy (IR) [4] and X-ray radial distribution function [5] studies on $50PbO–50V_2O_5$ glasses have concluded that the glass contains only VO_5 units. A neutron diffraction study [6] on a $41PbO–59V_2O_5$ glass came to a similar conclusion that the network consists of VO_5 tetragonal pyramids. A more recent IR study [7] of lead vanadate glasses indicated that the glass network structure is made up of unaffected VO_5 groups as in crystalline V_2O_5 and affected VO_5 groups as in crystalline $Pb(VO_3)_2$. However, a study on lead vanadate glasses using a combination of IR and static and magic angle spinning nuclear magnetic resonance (MAS-NMR) [8] arrived at a different conclusion for the local structure. The local vanadate structure for $x \leqslant 0.5$ consisted of both VO_5 trigonal bipyramids and VO_4 tetrahedra which are composed of $V_2O_7^{4-}$, $(VO_3)_n$ single chains, branched VO_4, and $(V_2O_8)_n$ zigzag chains depending on the PbO content. For the highest PbO content, the glass mainly consisted of VO_4 tetrahedra composed of $V_2O_7^{4-}$ and $(VO_3)_n$ single chains. PbO_3 trigonal pyramids and PbO_4 square pyramids are determined to be the local structure around the Pb atoms in these lead vanadate glasses. Thus, there remains some uncertainty as to the local structure in the lead vanadate glasses from these various studies.

As alluded to previously, XPS has proved to be an important tool in the study of the local structure of oxide glasses [9] as it can distinguish between bridging oxygen (BO) and non-bridging oxygen (NBO) [10,11] and even determine the concentration of a particular oxidation state of the transition metal(s) in the glass [12–14]. Moreover, since XPS has been successfully used to investigate the local structure in silicate glasses containing PbO, an XPS investigation of the lead vanadate glass system should be beneficial in elucidating the local structure in these vanadate glasses. The Pb 4f and O 1s spectra should be able to distinguish between the different roles that lead and oxygen play in the glass network structure. Also the V 2p spectra can provide information about the concentration of the various oxidation states of the vanadium anions. Magnetic susceptibility results will also be presented in order to provide an independent measure of the relative amounts of the different valence states of vanadium as well as to characterize the nature of any magnetic interaction between the magnetic species in these glasses.

2. Experimental details

2.1. Sample preparation

The glass samples were prepared using commercially available reagent grade powders of PbO and V_2O_5. Calculated amounts of these powders for $x = 0.2$, 0.3, 0.4, and 0.5 were mixed and melted in alumina crucibles at 1200 °C for 1 h. The glass, obtained by fast quenching of the melt, was cast into preshaped graphite-coated steel molds yielding rod specimens with dimensions $5 \times 5 \times 30$ mm^3. After casting, the specimens were transferred to another furnace maintained at 50 °C below the glass transition temperature (as determined from the differential thermal analysis) for 2 h and then cooled to room temperature at a rate of 30 °C/h. X-ray powder diffraction analysis indicated that the glasses were completely amorphous. After preparation, the samples were stored in a desiccator to prevent any further oxidation or degradation. The chemical compositions of the samples were determined by inductively coupled plasma emission spectroscopy (ICP) and are listed in Table 1. It should be noted that no trace of alumina was detected by the ICP technique indicating

Table 1
Nominal and analytic composition of $x\mathrm{PbO}\cdot(1-x)\mathrm{V_2O_5}$ glass samples

Nominal composition (mol%)		Analytic composition (mol%)		x
PbO	V_2O_5	PbO	V_2O_5	
0.20	0.80	0.22	0.78	0.22
0.30	0.70	0.35	0.65	0.35
0.40	0.60	0.43	0.57	0.43
0.50	0.50	0.54	0.46	0.54

The relative uncertainty in the ICP results is ±5%.

that the glasses did not react with the crucible during the melting process.

2.2. XPS measurements

The XPS experiments were carried out in a spectrometer equipped with a dual aluminum-magnesium anode X-ray gun and a 150-mm concentric hemispherical analyzer. Photoelectron spectra from Pb 4f, V 2p, O 1s, and C 1s core levels were recorded using a computer-controlled data collection system described elsewhere [15]. X-ray photoemission measurements were performed using non-monochromatic Al K_α (1486.6 eV) radiation from an anode operating at 130 W. The energy scale of the spectrometer was calibrated with the Cu $2p_{3/2}$ (= 932.67 eV), Cu $3p_{3/2}$ (= 74.9 eV), and Au $4f_{7/2}$ (= 83.98 eV) photoelectron lines. The electron energy analyzer was operated with a pass energy of 10 eV for the high-resolution XPS studies with an analyzer energy resolution of 1.0 eV, whereas a pass energy of 50 eV was used for routine survey scans.

For XPS measurements, a glass rod from each composition was cleaved in the analysis chamber at a base pressure 2×10^{-9} mbar before being transferred to the analysis chamber where the pressure was maintained at $<2\times10^{-10}$ mbar. The glass bars were notched to guide the fracture, yielding flat uncontaminated surfaces. Since XPS is sensitive to surface contamination, each sample was fractured in this manner as fracturing in UHV is considered to be the optimum method for producing a clean surface. For consistency, all binding energies are reported with reference to the C 1s transition at 284.6 eV, which arises from minor hydrocarbon contaminants in the vacuum and is generally accepted to be independent of the chemical state of the sample under investigation.

All spectra reported have been corrected for the charging effect and show the raw data as collected. A non-linear, least-squares algorithm [15] determine the best fit to each of the Pb 4f, O 1s, and V 2p spectra with either a single Gaussian–Lorentzien curve or two Gaussian–Lorentzien curves representing two different coordination geometries for lead, bridging and non-bridging oxygen, and two possible vanadium oxidation states (V^{5+} and V^{4+}), respectively. The fraction of non-bridging oxygen and V^{4+} were determined from the respective area ratios from these fits. Additional samples for each composition were analyzed in this manner and the quantitative XPS analysis of Pb 4f, O 1s, and V 2p were reproducible to ±5% with the overall accuracies in the determination of the peak position and chemical shift being 0.2 eV. A period of approximately 2 h was required to collect the data set for each sample and there was no evidence of any X-ray induced reduction of the vanadium or lead in the glasses during this period.

2.3. Magnetic measurements

The temperature-dependent dc magnetic susceptibility was measured using a Quantum Design SQUID magnetometer (model MPMS-5S) in a magnetic field of 5000 Oe over a temperature range of 5–300 K. The susceptibility of the sample holder is negligible below 100 K for all samples and constitutes less than a 2% correction at the highest temperature for all samples. The overall accuracy of the magnetic measurements is estimated to be approximately 3% due to the uncertainty of the magnetometer calibration.

3. Results

3.1. Survey scans

Relatively low-resolution X-ray photoelectron survey scans taken from fractured surfaces in the binding energy region 0–1200 eV were recorded for each glass sample and two such spectra are shown in Fig. 1. While a small C 1s core level peak arising from hydrocarbon contamination in the analysis chamber is observable, no aluminum signal is detected in these spectra which provides additional evidence that the glass did not react with the alumina crucible during the melting process. Each spectrum includes the photoelectron and X-ray induced Auger peaks from the constituent elements of the glass. It is clear from these spectra that the Pb 4f core level doublet increases in intensity with increasing PbO content in the glass while that of the V 2p core level decreases relative to the Pb 4f peak. Each core level peak of interest, i.e., Pb 4f, O 1s, and V 2p, was also recorded under high-resolution conditions and are presented in the next sections.

3.2. Lead spectra

The high-resolution Pb 4f spin–orbit doublet spectra for all the glass samples are collectively shown in Fig. 2. The peak positions of the spin–orbit doublet Pb $4f_{5/2}$ and Pb $4f_{7/2}$ for these lead vanadate glasses are in excellent agreement with the corresponding values of 143.4 eV ($4f_{5/2}$) and 138.6 eV ($4f_{7/2}$) reported for PbO [16]. Qualitatively, the binding energies (BE) of these two peaks decreases with increasing PbO content while the intensities of the peaks and the full-width at half-maximum (FWHM) increase. As no clear asymmetry could be found in either of the two peaks in

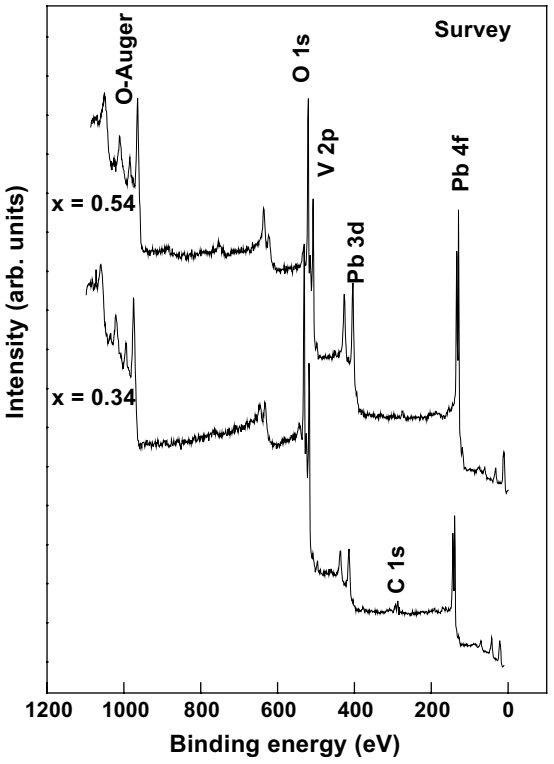

Fig. 1. Survey scans of the XPS spectra for PbO vanadate glass samples with $x = 0.35$ and 0.54.

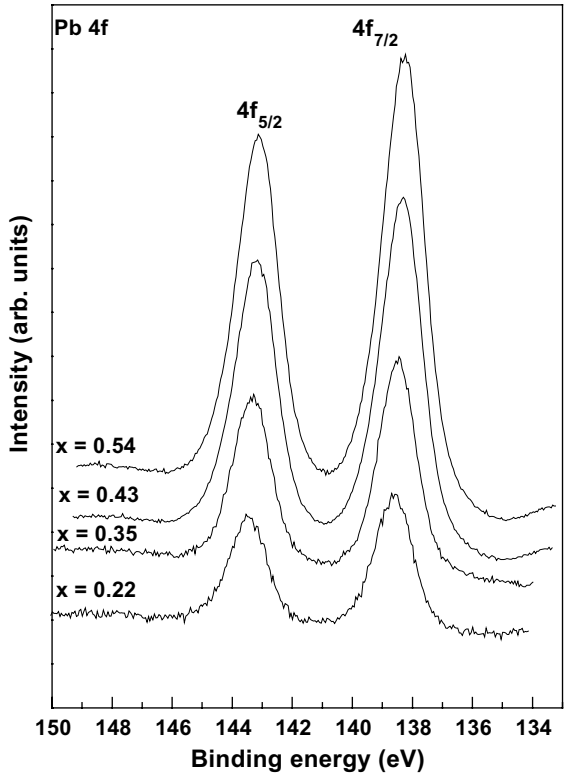

Fig. 2. High-resolution Pb 4f spectra for all four $x\mathrm{PbO}\cdot(1-x)\mathrm{V_2O_5}$ glass samples.

each spectrum, the Pb $4f_{5/2}$ and Pb $4f_{7/2}$ peaks are each fitted to a single Gaussian–Lorentzian curve.

3.3. Oxygen spectra

The O 1s core level high-resolution spectra for the $0.22 \leqslant x \leqslant 0.54$ glasses displayed in Fig. 3 show a single peak for all glasses samples. In addition to the observation that the O 1s peaks for the glasses shift towards lower binding energy with increasing lead oxide content, the peak intensity also decreases slightly. This decrease in the peak intensity can be easily understood by the fact that the replacement of V_2O_5 by PbO should lead to a decrease in the total number of oxygen atoms in the glass, and therefore a decrease in the intensity of the O 1s signal. In addition, a slight asymmetry in the O 1s core level peak is apparent in several of the spectra, which is indicative of two different types of oxygen sites in these glasses. Consequently, all O 1s spectra were fitted to two Gaussian–Lorentzian peaks in order to determine the peak positions and relative abundance of the different oxygen sites.

3.4. Vanadium spectra

Fig. 4 shows the high-resolution V 2p spin–orbit doublet spectra for the lead vanadate glass samples. The peak intensity decreases with increasing PbO content in these glasses, while the peak position and width of the V $2p_{3/2}$ peak at ~517 eV do not vary much with composition. Although the V $2p_{3/2}$ peaks are rather narrow for all glass samples, a closer inspection of the V $2p_{3/2}$ peak reveals a slight asymmetry toward the low binding energy (BE) side of the core level peak for the $x = 0.22$ and 0.35 glass samples. Since this asymmetry is indicative of V existing in more than one oxidation

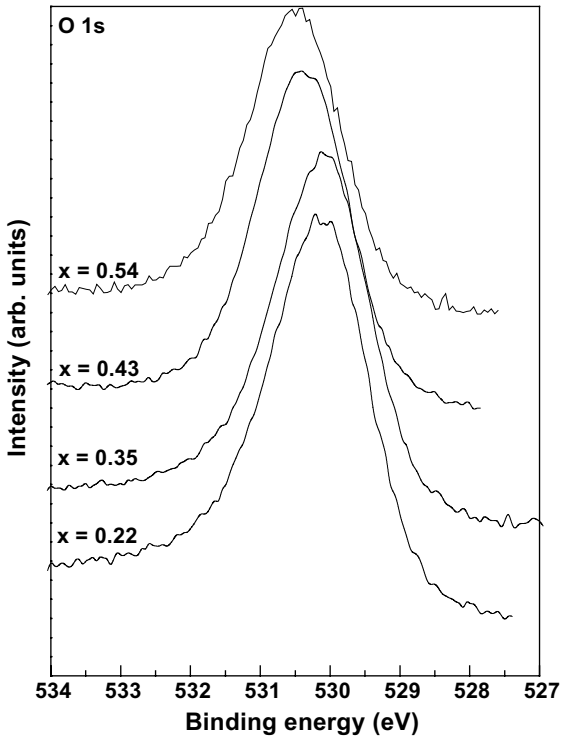

Fig. 3. High-resolution O 1s spectra for all four xPbO·$(1-x)V_2O_5$ glass samples.

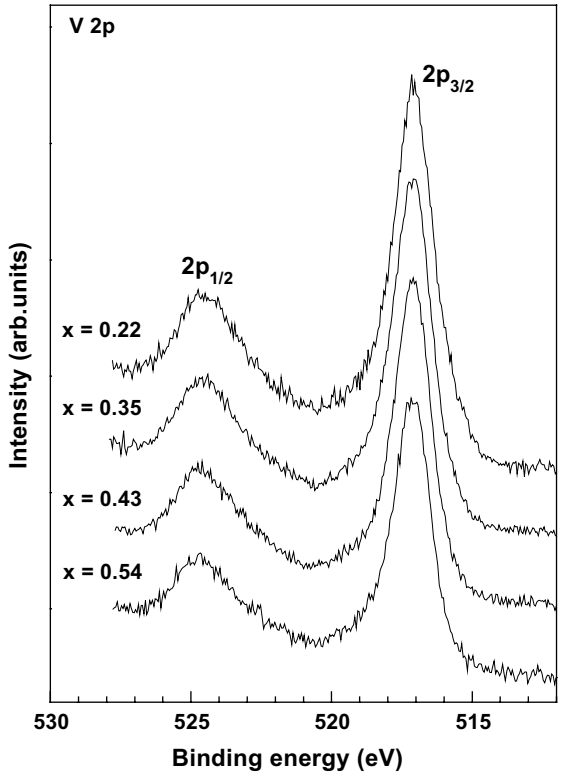

Fig. 4. High-resolution V 2p spectra for all four xPbO·$(1-x)V_2O_5$ glass samples.

state for these two glass samples, these spectra were subsequently fitted to two Gaussian–Lorentzian peaks. The V $2p_{3/2}$ peaks for the glass samples with $x \geqslant 0.43$ are very symmetric as no shoulder or asymmetry could be seen in these two spectra and correspondingly they are fitted with a single Gaussian–Lorentzian curve.

3.5. Magnetic susceptibility measurements

The magnetic susceptibility results for these glasses are displayed in Fig. 5 as plots of the inverse of the magnetic susceptibility, M/H, as a function of the temperature T. The susceptibility data do not appear to follow a Curie–Weiss behavior ($M/H = C/(T-\theta)$) as the susceptibility becomes nearly temperature independent in the high temperature region (200–300 K). After attempting several other fitting possibilities, it was found that the data for each sample could be satisfactorily fitted to a positive temperature-independent constant plus a Curie–Weiss like temperature-dependent contribution. The temperature-independent constants are determined from a high-temperature extrapolation of M/H-vs-$1/T$ plots for temperatures above 200 K (see Fig. 6) After subtracting these temperature-independent constants from the measured susceptibility data,

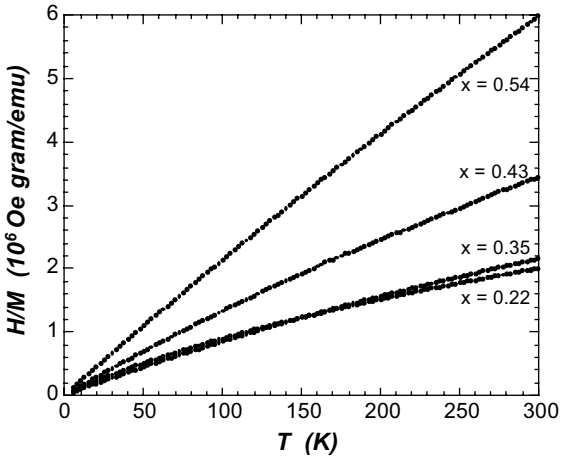

Fig. 5. The inverse of the mass magnetic susceptibility M/H as a function of temperature T for the $x\mathrm{PbO}\cdot(1-x)\mathrm{V_2O_5}$ glass samples in a magnetic field of 5000 Oe.

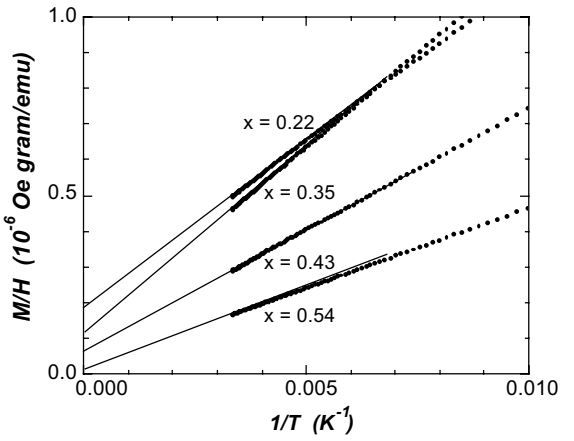

Fig. 6. Magnetic susceptibility-versus-inverse temperature for PbO vanadate glasses. Solid lines are high-temperature extrapolations with the intercept representing $(M/H)_{\text{constant}}$.

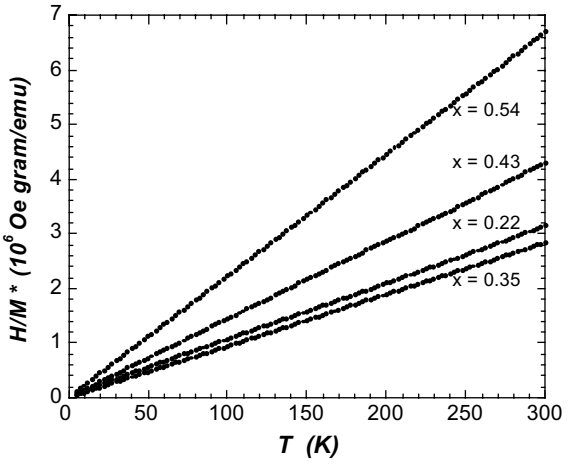

Fig. 7. The inverse of the 'corrected' magnetic susceptibility ($M^*/H = M/H - (M/H)_{\text{constant}}$) as a function of temperature for the PbO vanadate glasses.

the resulting M^*/H ($= M/H - (M/H)_{\text{constant}}$) data follow a Curie–Weiss behavior ($M^*/H = C/(T-\theta)$) as shown in Fig. 7 with the Curie constant C and the paramagnetic Curie temperature θ determined from least-square fits of the H/M^*-vs-T data. These three parameters (($M/H)_{\text{constant}}$, C, and θ) determined from this fitting procedure are displayed in Table 2 for each of the glass samples.

Table 2
Magnetic susceptibility results for the $x\mathrm{PbO}\cdot(1-x)\mathrm{V_2O_5}$ glass samples and the concentration of V^{4+} ions to total vanadium ions

x	$(M/H)_{\mathrm{constant}}$ (10^{-7} emu/Oe g)	C (10^{-7} emu/Oe g)	θ	$[V^{4+}]/[V_{\mathrm{total}}]$
0.22	1.81	9.67	−4.16	3.15
0.35	1.11	10.57	−0.79	4.25
0.43	0.575	6.99	−1.44	3.26
0.54	0.178	4.48	−0.21	2.65

The experimental uncertainty in the magnetic determinations is ±3%.

4. Discussion

As described in the preceding section, the peak positions of the Pb $4f_{5/2}$ and Pb $4f_{7/2}$ core levels decrease while their FWHM increase with increasing PbO content. (See Table 3 for values of the binding energies and corresponding FWHM based on a single Gaussian–Lorentzian curve fit to each Pb 4f peak.) Since changes in the binding energy are associated with a change in the local chemical environment, the decrease in the BEs of the Pb 4f core levels results from an increase in the effective electronic charge density around the Pb atoms due a change in the type of PbO_n polyhedra present or a change in the role of Pb in the glass network structure. Network structural terms such as glass former and modifier are just a reflection of this electron localization. A modifier cation typically has a low electronegativity and forms an ionic bond as electronic charge is transferred to the neighboring oxygen. This electron transfer decreases the electron density of the cation and correspondingly increases the electron binding energy. On the other hand, a glass former has a relatively higher electronegativity such that the bond to oxygen is more covalent, which constrains the electron density to the region between the atoms. This results in an enhancement of the average electron density on the cation and a corresponding decrease in its electron binding energy. Therefore the gradual decrease in binding energies of the Pb 4f levels with increasing PbO is consistent with a gradual transition in the nature of the Pb–O bond from ionic to covalent. In addition, the intensities of both P 4f peaks increase at a rate faster than a linear dependence on the Pb concentration indicating that the average Pb electron density is increasing and becoming more covalent in nature. Similarly, the increase in the FWHM of both Pb 4f peaks from 1.5 eV for the two smaller PbO containing glasses ($x \leqslant 0.35$) to 1.7 eV for the two larger PbO containing glasses is in accordance with this speculation. More definitive evidence for this change in the role of Pb from a glass modifier to a glass former would be the appearance of an asymmetry in the Pb 4f peaks as the binding energies for each role should be different. As seen in Fig. 8, however, very good fits to each of the Pb 4f peaks can be accomplished by a single Gaussian–Lorentzian curve for both the $x = 0.35$ glass sample as well as the $x = 0.54$ glass sample. Thus any shift in the binding energy from an ionic Pb–O bond to a more covalent Pb–O bond is below the resolution of the present XPS measurements. Likewise, the XPS resolution is insufficient to distinguish between the PbO_3 trigonal and PbO_4

Table 3
Peak positions, FWHM, and peak separation from the curve fittings of the Pb $4f_{5/2}$ and Pb $4f_{7/2}$ core levels for the PbO vanadate glasses

x	Pb $4f_{5/2}$ (eV)	FWHM (eV)	Pb $4f_{7/2}$ (eV)	FWHM (eV)	$\Delta E_{\mathrm{Pb}\,4f5/2-\mathrm{Pb}\,4f7/2}$ (eV)
0.22	143.47	1.54	138.62	1.53	4.85
0.35	143.44	1.56	138.58	1.52	4.86
0.43	143.28	1.70	138.43	1.68	4.85
0.54	143.18	1.74	138.33	1.74	4.85

The experimental uncertainty in the energy measurements is ±0.2 eV.

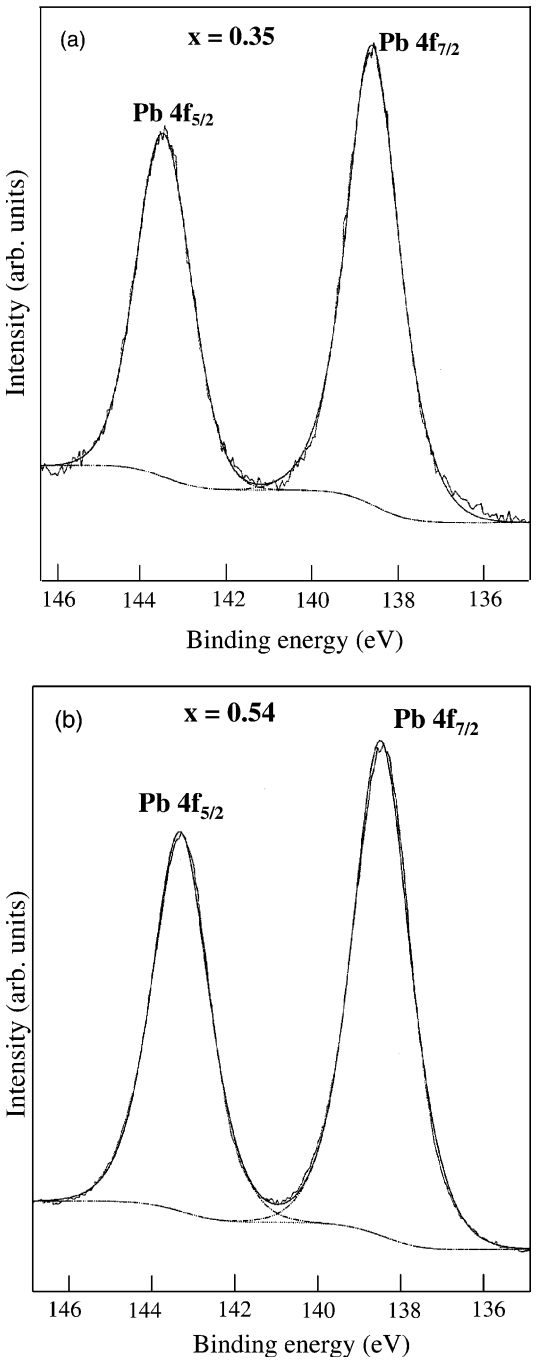

Fig. 8. High-resolution Pb 4f spectra for (a) $x = 0.35$ and (b) 0.54 PbO vanadate glass samples and the resulting single Gaussian–Lorentzian peak (smooth line) from the least-squares fitting routine. The smooth solid line is the resultant sum of fitting both Pb 4f peaks simultaneously.

square pyramid structures suggested to be present in these lead vanadate glasses from previous NMR studies [2].

In most XPS studies of oxide glasses, the O 1s spectra are more informative with respect to the structure of the glass than the cation (Pb) spectra. Specifically, the binding energy of the O 1s electrons is a measure of the extent to which electrons are localized on the oxygen or in the internuclear region, a direct consequence of the nature of the bonding between the oxygen and different cations. As a small asymmetry was observed in the high-resolution O 1s spectra, all O 1s spectra were fitted to two Gaussian–Lorentzian peaks. This fitting procedure resulted in two distinct, but overlapping peaks for the glasses with $x \leqslant 0.43$ while the fitting software would always converge to a single peak for the O 1s spectra of the $x = 0.54$ glass sample as seen in Fig. 9. (See Table 4 for numerical values resulting from the fits.) Owing to the higher BE peak indicating a smaller electron density at the oxygen site, this peak is associated with a 'bridging oxygen' (BO) atom of the V–O–V configuration while the lower BE peak is associated with 'non-bridging oxygen' (NBO) sites having V–O–Pb, Pb–O–Pb, and V=O configurations. This assignment is similar to those of an earlier XPS study on lead silicate glasses [2].

The change in the relative concentration of NBO versus PbO content is also consistent with this O 1s peak assignment, as the number of BO sites (V–O–V bonds) should gradually decrease with increasing PbO content. Assuming that vanadium ions enter the glass network just as a trigonal bipyramid (VO_5) structure with three BO and two NBO per vanadium ion, the number of NBO can be quantitatively determined from

$$\frac{\mathrm{NBO}}{\mathrm{TO}} = \frac{4(1-x)+x}{5-4x} = \frac{4-3x}{5-4x}, \tag{1}$$

where TO represents the total oxygen content in the glass. Table 4 shows that while the experimental NBO/TO ratio increases from 81% to 92% with increasing PbO, the calculated ratio from Eq. (1) ranges between 81% and 83%. This small underestimation indicates that other VO_n polyhedra could be present, especially as the PbO content approaches 50 mol% in these vanadate glasses.

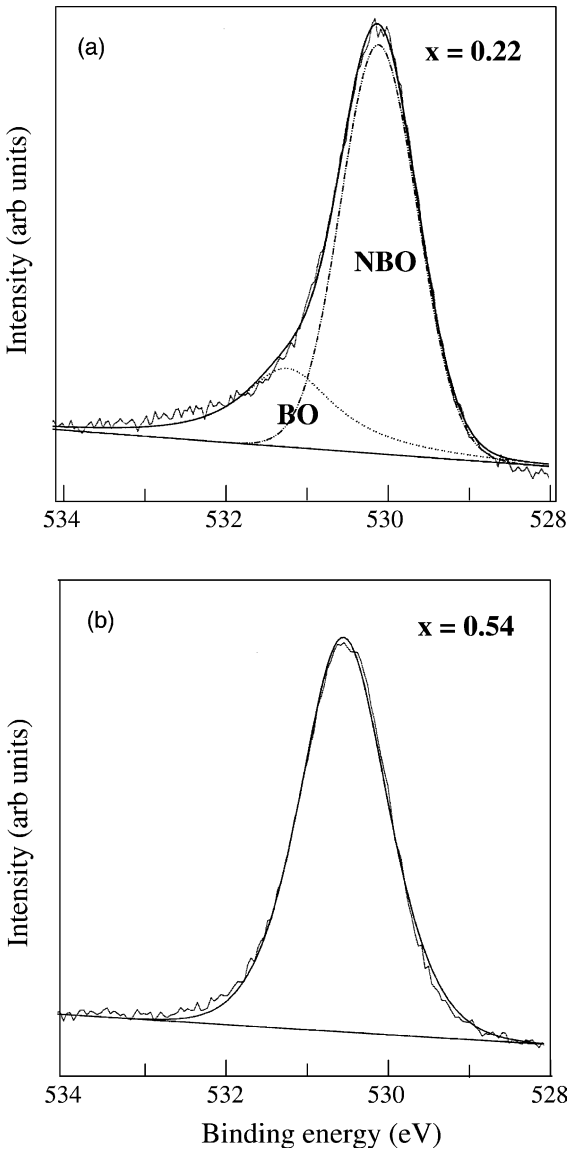

Fig. 9. (a) High-resolution O 1s spectrum for the $x = 0.22$ PbO vanadate glass sample and the resulting NBO and BO peaks (dotted and dashed lines) from the least-squares fitting routine. (b) High-resolution O 1s spectrum for the $x = 0.54$ PbO vanadate glass sample and the resulting single peak (smooth line) from the least-squares fitting routine.

According to the IR and NMR structural studies on lead vanadate glasses [8], both VO_5 trigonal bipyramids and VO_4 tetrahedra are present for the $x \leqslant 0.5$ glasses while higher PbO concentrated glasses consist mainly of VO_4 tetrahedra. Assuming that all oxygen sites for the VO_4 tetrahedra are NBO, then the difference in the experimental NBO/TO ratios and those determined from just VO_5 trigonal bipyramids could be accounted for by VO_4 tetrahedra (100% NBO) replacing the VO_5 trigonal bipyramids (~80% NBO) with increasing PbO.

The appearance of a single, symmetric peak in the O 1s spectrum for the $x = 0.54$ glass indicates that all oxygen bonds (V–O–V, V–O–Pb, Pb–O–Pb) must have essentially the same binding energy. Correspondingly, the effective electron density surrounding each oxygen anion must be very similar. Thus the most plausible explanation for an identical electron density for these differing types of bonds is if the oxygen bonds are more covalent than ionic in nature. This would be consistent with PbO becoming a glass former for $x > 0.5$.

Although vanadium can exist in more than one oxidation state, the observation that the peak position and the width of the V $2p_{3/2}$ peak do not change appreciably with the PbO content in these glasses (see Table 5) suggest that one oxidation state of vanadium is predominant in these glasses. It is known [17,18] that the core level spectrum of V^{4+} has a $2p_{3/2}$ binding of 515.95 eV while the core level spectrum of V^{5+} has a $2p_{3/2}$ binding energy of 517.2 eV for vanadium oxides. Thus deconvoluting the V $2p_{3/2}$ core level peak into two contributions with an energy separation of ~1.25 eV should permit a more quantitative estimate of the ratio of V ions in V^{4+} and V^{5+} states. Two Gaussian–Lorentzian peaks centered at approximately 515.9 and 517.2 eV are subsequently fitted to the experimental data. Figs. 10(a) and (b) show the V $2p_{3/2}$ high-resolution spectra for the $x = 0.35$ and 0.54 glass samples. It is found that the V $2p_{3/2}$ core level peak for the glass with composition $x = 0.35$ can be satisfactorily fitted with two Gaussian–Lorentzian peaks, one centered at 517.14 eV corresponding to a contribution from V^{5+} ions, and the other centered at 515.82 eV corresponding to a contribution from V^{4+} ions. However, the V $2p_{3/2}$ core level peak for the glass composition $x \geqslant 0.43$ can be easily fitted with only one peak at a binding energy of 517.10 eV, which would correspond to a contribution solely from the V^{5+} ions. Thus there would be negligible V^{4+}

Table 4
Peak positions, FWHM, peak separation, and relative concentration of NBO resulting from the curve fittings of the O 1s core level for the PbO vanadate glasses

x	O 1s (eV)		FWHM (eV)		ΔE_{BO-NBO} (eV)	[NBO]/[TO] (%)	
	BO	NBO	BO	NBO		Measured	Eq. (1)
0.22	531.66	529.95	3.10	1.65	1.71	81	81
0.35	531.31	529.98	2.33	1.58	1.32	88	82
0.43	530.92	530.08	1.62	1.47	0.84	92	83
0.54	530.15[a]		1.63[a]				

The experimental uncertainty in the energy measurements is ±0.2 eV.
[a] The single O 1s peak for $x = 0.54$ is associated with all oxygen bonds having essentially the same binding energy.

Table 5
Peak positions, FWHM, peak separation, and relative concentration of V^{4+} resulting from the curve fittings of the V $2p_{3/2}$ core level for the PbO vanadate glasses

x	V $2p_{3/2}$ (eV)		FWHM (eV)		$\Delta E_{V^{5+}-V^{4+}}$ (eV)	$[V^{4+}]/[V_{total}]$ (%)
	V^{5+}	V^{4+}	V^{5+}	V^{4+}		
0.22	517.08	515.82	1.70	1.60	1.26	4.1
0.35	517.14	515.89	1.70	1.65	1.25	3.7
0.43	517.10	–	1.57	–	–	0.0
0.54	517.05	–	1.57	–	–	0.0

The experimental uncertainty in the energy measurements is ±0.2 eV.

ions present in these higher concentrated PbO vanadate glasses. Ratios of the relative areas under the fitted V^{5+} and V^{4+} peaks provide a measure of the relative concentration of the two V ions and are summarized in Table 5. Thus even for the smaller PbO containing glass samples, only about 4% of the vanadium atoms are in the V^{4+} oxidation state, which has a non-zero magnetic moment.

As described previously, the best fit to the magnetic susceptibility data was found to consist of a positive temperature-independent term plus a Curie–Weiss-like temperature-dependent behavior. The temperature-independent term can be understood in terms of two contributions: a diamagnetic one arising from the core ions in the glass matrix, and a temperature-independent paramagnetic contribution arising from the presence of V_2O_5 in vanadate glasses ($\sim 5\times 10^{-7}$ emu/Oe g V_2O_5) [19]. Thus, the temperature-independent susceptibility (a constant background) can be either positive or negative depending on the relative size of these two contributions. In these glasses the paramagnetic V_2O_5 contribution dominates the core diamagnetic contribution arising from Pb, O, and V, such that the resulting background is positive. Moreover, the linear decrease in the $(M/H)_{constant}$ values with increasing PbO content is consistent with the temperature-independent paramagnetic V_2O_5 contribution decreasing with decreasing V_2O_5 content. On the other hand, the Curie temperature-dependent behavior observed in these glasses must be associated with a fraction of the vanadium ions being in another oxidation state other than V^{5+} since V^{5+} ions are non-magnetic. The most probable oxidation state is V^{4+} which has a magnetic moment, $p_{eff} = 1.73\mu_B$. Thus, from the Curie constant C in conjunction with the vanadium concentration determined by chemical analysis on these oxide glasses, 2.5–4.0% of the total V concentration for these glasses are in the V^{4+} state as shown in Table 2. These very low percentages are consistent with XPS determinations from the V 2p spectra as well as with the V^{4+} concentrations determined from susceptibility results on lead silicate glasses [20]. The negative paramagnetic Curie temperature values in the range of −0.2 to −4.2 K indicate a weak antiferromagnetic interaction between the V^{4+} ions. These small values are not surprising since θ is proportional to the number of neighboring

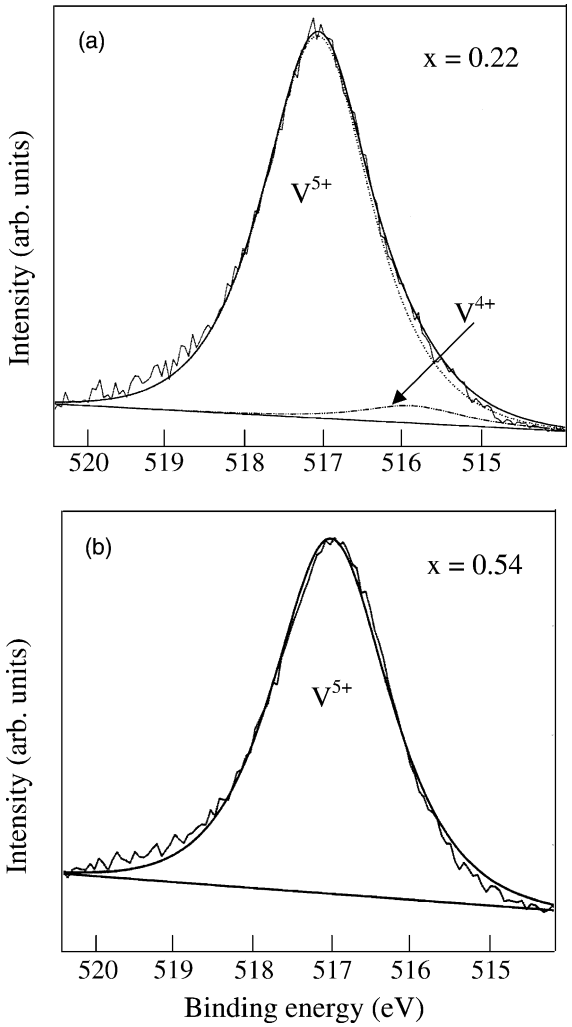

Fig. 10. (a) High-resolution V $2p_{3/2}$ spectrum for the $x = 0.22$ PbO vanadate glass sample and the resulting V^{5+} and V^{4+} peaks (dotted and dashed lines) from the least-squares fitting routine. (b) High-resolution V $2p_{3/2}$ spectrum for the $x = 0.54$ PbO vanadate glass sample and the resulting single V^{5+} peak (smooth line) from the least-squares fitting routine.

magnetic ions (negligible for these low V^{4+} concentrations) as well as the strength of the magnetic interaction.

5. Conclusions

XPS and magnetic susceptibility studies were used to investigate the structural and the magnetic properties of the lead vanadate glasses. It was found that the polarizability of Pb is concentration dependent and grows with increasing PbO content in the vanadate glasses. At low PbO content, V_2O_5 acts as the glass former while PbO behaves like a glass modifier with over 80% of the oxygen being in non-bridging oxygen sites. For $x > 0.5$, all oxygen bonds have essentially the same binding energy indicating that all oxygen in the glass network are covalently bonded and that the role of PbO switches from that of a glass modifier to that of a glass former. The decrease in the binding energies for both Pb $4f_{7/2}$ and Pb $4f_{5/2}$ core levels, the increase in intensities of both peaks, and the increase in the peaks' FWHM with increasing PbO content are also consistent with this change in the structural role of PbO from a glass modifier to glass former for $x > 0.5$. Vanadium is found to be predominantly in the V^{5+} state for $x \leqslant 0.35$ glasses, while no V^{4+} ions are detectable in the XPS spectra for the $x \geqslant 0.43$ glasses. V^{4+} concentrations of about 4% are in good agreement with the determinations from magnetic susceptibility results. The magnetic behavior of these glasses consists of a Curie–Weiss temperature-dependent behavior from the V^{4+} ions plus a positive temperature-independent contribution from V_2O_5.

Acknowledgements

Two of the authors (A.M. and G.D.K) would like to thank King Fahd University of Petroleum and Minerals (KFUPM) and the Physics Department at KFUPM for support. Also the assistance of Dr P.S. Fodor with the magnetic susceptibility measurements is greatly appreciated.

References

[1] B.M.J. Smets, T.P.A. Lommen, J. Non-Cryst. Solids 48 (1982) 423.
[2] P.W. Wang, L. Zhang, J. Non-Cryst. Solids 194 (1996) 129.
[3] I.A. Gee, D. Holland, C.F. McConville, Phys. Chem. Glasses 42 (2001) 339.
[4] V. Dimitrov, Y. Dimitriev, J. Non-Cryst. Solids 122 (1990) 133.
[5] V. Fares, M. Magini, A. Montenero, J. Non-Cryst. Solids 99 (1988) 404.

[6] A.C. Wright, C.A. Yarker, P.A.V. Johnson, J. Non-Cryst. Solids 76 (1985) 333.
[7] S. Mandel, A. Ghosh, Phys. Rev. B 48 (1993) 9388.
[8] S. Hayakawa, T. Yoko, S. Sakka, J. Non-Cryst. Solids 183 (1995) 73.
[9] C.G. Pantano, in: Experimental Techniques of Glass Science, American Ceramic Society, Westerville, OH, 1993, p. 129.
[10] B.M.J. Smets, T.P.A. Lommen, J. Non-Cryst. Solids 46 (1981) 21.
[11] B.M.J. Smets, D.M. Krol, Phys. Chem. Glasses 25 (1984) 113.
[12] A. Mekki, D. Holland, C.F. McConville, M. Salim, J. Non-Cryst. Solids 208 (1996) 267.
[13] A. Mekki, D. Holland, C.F. McConville, J. Non-Cryst. Solids 215 (1997) 271.
[14] A. Mekki, D. Holland, Kh.A. Ziq, C.F. McConville, J. Non-Cryst. Solids 272 (2000) 179.
[15] E.E. Khawaja, Z. Hussain, M.S. Jazzar, O.B. Dabbousi, J. Non-Cryst. Solids 93 (1987) 45.
[16] W.E. Morgan, J.R. Van Wazer, J. Phys. Chem. 77 (1973) 964.
[17] E.Z. Kurmaev, V.M. Cherkashenko, Yu.M. Yarmoshenko, St. Bartkowski, A.V. Postnikov, M. Neumann, L.-C. Duda, J.H. Guo, J. Nordgren, V.A. Perelyaev, W. Reichelt, J. Phys.: Condens. Matter 10 (1998) 4081.
[18] M. Demeter, M. Neumann, W. Reichelt, Surf. Sci. 454–456 (2000) 41.
[19] Y. Kawamota, J. Tanida, H. Hamada, H. Kiriyama, J. Non-Cryst. Solids 38&39 (1980) 301.
[20] S. Sen, A. Ghosh, J. Mater. Res. 15 (2000) 995.